DEC 27 1949 REC'D

CLASSIFICATION [redacted] CANCELLED

Copy /
RM SL9L1[illegible]

[redacted]

NACA

CLASSIFICATION CANCELLED

RESEARCH MEMORANDUM

for the

Ordnance Department, Department of the Army

FLIGHT TEST OF THE AEROJET 7KS-6000 T-27

JATO ROCKET MOTOR

By Aleck C. Bond and Joseph G. Thibodaux, Jr.

Langley Aeronautical Laboratory
Langley Air Force Base, Va.

CLASSIFICATION CANCELLED

[redacted] J.W. Crowley [redacted] 4/1/55

[redacted]

OES

Status: [redacted]

NACA Change # 2907

NATIONAL ADVISORY COMMITTEE
FOR AERONAUTICS

WASHINGTON

DEC 20 1949

CLASSIFICATION [redacted] CANCELLED

NATIONAL ADVISORY COMMITTEE FOR AERONAUTICS

RESEARCH MEMORANDUM

for the

Ordnance Department, Department of the Army

FLIGHT TEST OF THE AEROJET 7KS-6000 T-27 JATO ROCKET MOTOR

By Aleck C. Bond and Joseph G. Thibodaux, Jr.

SUMMARY

A flight test of the Aerojet Engineering Corporation's 7KS-6000 T-27 Jato rocket motor was conducted at the Langley Pilotless Aircraft Research Station at Wallops Island, Va. to determine the flight-performance characteristics of the motor. The flight test imposed an absolute longitudinal acceleration of 9.8g upon the rocket motor at 2.8 seconds after launching. The total impulse developed by the motor was 43,400 pound-seconds, and the thrusting time was 7.58 seconds. The maximum thrust was 7200 pounds and occurred at 4.8 seconds after launching. No thrust irregularities attributable to effects of the flight longitudinal acceleration were observed. Certain small thrust irregularities occurred in the flight test which appear to correspond to irregularities observed in static tests conducted elsewhere. A hypothesis regarding the origin of these small irregularities is presented.

INTRODUCTION

The Aerojet 7KS-6000 T-27 Jato rocket motor was developed by the Aerojet Engineering Corp. under the supervision of the Air Materiel Command and the Office of Chief of Ordnance as a solid-propellant, medium-duration, low-acceleration booster for NACA pilotless-aircraft research models. As part of the evaluation of this rocket motor it was desirable to determine its performance in flight as well as in static thrust-stand tests. Accordingly, a flight test of this motor has been conducted at the Langley Pilotless Aircraft Research Station at Wallops Island, Va. The results of this test are given in the present paper in correlation with results of static tests by the manufacturer and the Aberdeen Proving Ground.

The static tests of the motor performed by the manufacturer and the Aberdeen Proving Ground indicated that the motor functioned satisfactorily during static firing. Such static tests yield internal ballistic data and time histories of pressure and thrust; however, these tests are inadequate for evaluation of the flight performance of the motor, as they do not indicate the effects of acceleration in free flight on the various components of the motor.

The components most likely to be affected by acceleration in a solid-propellant rocket motor are the powder trap and the propellant. Failure of either of these components may lead ultimately to case failure due to high internal pressures resulting from blocking of the nozzle or increased propellant burning area.

SYMBOLS

a — longitudinal acceleration with respect to the ground, feet per second per second

C_D — drag coefficient $\left(\frac{D}{qS}\right)$

D — drag, pounds

g — acceleration due to gravity, 32.17 feet per second per second

t — time from instant of ignition, seconds

T — thrust, pounds

W — weight, pounds

γ — flight-path angle, degrees

S — cross-sectional area, square feet

q — dynamic pressure, pounds per square foot $\left(\frac{1}{2}\rho V^2\right)$

ρ — air density, slugs per cubic foot

V — velocity, feet per second

DESCRIPTION OF THE ROCKET MOTOR

The Aerojet 7KS-6000 T-27 Jato rocket motor as supplied by the manufacturer is shown in figure 1(a). A complete breakdown of all the component parts of the motor is shown in figure 1(b). The motor utilizes two single-perforated cylindrical propellant grains. The propellant is composed of an ammonium perchlorate oxidizer bound in a matrix of thermosetting resin fuel. The ends of the grain are restricted by a thermosetting resin backed with tar paper. The two grains are supported in the case by means of three trap plates held together by a rod passing through the central perforation of the grain. Inertia, viscous, and pressure forces are transmitted to the rear trap assembly, which is supported on steel legs welded to the nozzle entrance cone, and through the center trap assembly and tie rod to the boss in the front of the chamber. The loaded weight of the motor was 527.75 pounds. The empty weight of the motor was 317.25 pounds. A more detailed description of the motor can be found in reference 1.

DESCRIPTION OF THE MODEL

The external configuration of the test model equipped with four stabilizing fins and nose is shown in figure 2. The fins were flat plates having wedge leading edges of 28° total angle measured in the direction perpendicular to the leading edge and square trailing edges. The nose was a cone 18 inches long and $13\frac{3}{16}$ inches in diameter. Within the nose was mounted the telemeter together with sufficient lead ballast to bring the center of gravity to the positions shown in figure 2 in order to achieve sufficient aerodynamic stability. The gross weight of the model was 708 pounds. The propellant plus igniter weight was 210.5 pounds, so that the empty weight of the model was 497.5 pounds.

TEST APPARATUS AND INSTRUMENTATION

The Aerojet 7KS-6000 T-27 Jato rocket-motor flight model was launched from a near-zero-length, crutch-type launcher at an angle of 42.5° to the horizontal. The launcher consisted of a crutch-type wooden A-frame mounted on a T-shaped base. When mounted, the model was supported in front by the A-frame crutch and in the rear by means of a support under the nozzle. A photograph of the model on the launcher is shown in figure 3.

The model was instrumented with a standard NACA two-channel telemeter transmitting measurements of longitudinal acceleration from two accelerometers. One accelerometer covered the range from 20g acceleration to 1g deceleration, and the other accelerometer covered the range from 1g acceleration to 15g deceleration.

In addition to telemetered data, a time history of the flight velocity was obtained using a 100-watt continuous-wave Doppler radar unit. Time histories of range, azimuth, and elevation were obtained by means of a modified SCR-584 radar theodolite. Prevailing atmospheric conditions were obtained from a standard radiosonde released at the time of launching. A detailed description of the functioning of the CW Doppler radar and radio telemeter may be found in reference 2.

The launching of the rocket was photographed with two fixed line-of-sight Army K-24 type rapid recycling aerial cameras and a high-speed 35-millimeter Mitchell motion-picture camera in order to observe the operation of the launcher. Both the launching and the flight of the rocket were photographed with a tracking 16-millimeter Cine-Kodak motion-picture camera in order to provide qualitative information on the stability of the flight and possible correlation of the appearance of the rocket jet with any anomalies that might occur in the rocket performance.

RESULTS AND DISCUSSION

Velocity

The time history of the velocity obtained from the CW Doppler radar is presented in figure 4. The initial part of the curve was not obtained because of inability to track with radar equipment at close range. Zero time was established as the time when ignition began. The model reached a maximum velocity of 1525 feet per second, corresponding to a Mach number of 1.37.

Acceleration

The time history of the acceleration as obtained from telemetered data is presented in figure 5. The accelerations shown are absolute accelerations and include the component of gravity resulting from model attitude. The record indicates a short delay in the initial portion of the curve which corresponds to the ignition delay of the motor and then a rapid change in acceleration is observed which corresponds to motor thrust build-up. At 1.1 and 4.4 seconds sudden increases in acceleration take place, indicating an erratic increase in thrust.

A maximum acceleration of 9.8g is reached 2.8 seconds after launching. Burnout occurs at 7.58 seconds. A maximum deceleration of 7.3g is reached at 7.7 seconds. A complete time history of the acceleration was obtained for the total flight covering 17.3 seconds.

Drag Coefficient

Assuming that the angle of attack of the model is zero, the drag of the model during coasting flight may be obtained from the equation of motion

$$D = -W\left(\frac{a}{g} + \sin \gamma\right)$$

where $\frac{a}{g} + \sin \gamma$ is the absolute longitudinal acceleration as indicated directly by the accelerometer in g units. The assumption was made that the burnout weight of the model was equal to the initial weight of the model minus the propellant and igniter weight.

The time history of the altitude as obtained from the modified SCR-584 radar is shown in figure 6. The variation of air density and speed of sound with altitude as obtained from the radiosonde data is shown on figure 7. These data were used for conversion of drag into drag coefficient based on the maximum model cross-sectional area of 0.948 square foot. Drag coefficient plotted as a function of Mach number is shown in figure 8. Data were inadequate for obtaining drag coefficients below a Mach number of 0.67; hence, the curve was extrapolated for lower Mach numbers.

Thrust

The thrust may be determined from the drag and the absolute longitudinal acceleration by the following equation:

$$T = W\left(\frac{a}{g} + \sin \gamma\right) + D$$

where W is the instantaneous weight of the model in pounds. The propellant was assumed to be expended at a constant rate for a first approximation of thrust. A second approximation was computed, assuming a change of propellant weight proportional to thrust. It was assumed that at any given Mach number the model drag coefficient during the thrusting period was equal to the drag coefficient during the coasting period corrected for the pressure drag over the nozzle exit. Since no specific base-pressure data were available for this particular model, the data presented in reference 3 were used for an approximate correction to the drag. Thrust was not corrected for altitude since this correction was considered negligible for the altitudes attained by the model.

The resulting thrust-time curve, as obtained from computing instantaneous values of thrust at various times, is presented in figure 9. The preignition temperature of the propellant was 75° F. An ignition delay of 0.09 second is indicated by the record. A maximum thrust of 7200 pounds was reached at 4.8 seconds and the total burning time was 7.58 seconds. The total impulse of the rocket is 43,400 pound-seconds, giving a specific impulse value of 207 pound-seconds per pound of propellant. The thrust-time curve and specific-impulse value are in good agreement with data obtained in static firings by the manufacturer. Selected curves from static tests conducted by the manufacturer are shown in figures 10(a) and 10(b). Results from static test by the Aberdeen Proving Ground are presented in figure 11.

It will be noted in figures 9, 10(a), and 10(b) that the thrust changes erratically in the time region 0.7 to 1.8 seconds and again in the region from 4.0 to 5.2 seconds. These thrust irregularities are not characteristic of single-perforated cylindrical propellant grains. Since they occur in flight as well as in static tests, they cannot be attributed to flight effects.

A possible explanation of the origin of these thrust fluctuations is the following. The propellant grains are supported by being clamped between the three trap assemblies shown as parts 16, 17, and 18 in figure 1(b). The clamping action is provided by tension within the two tie rods connecting the trap assemblies, and possibly to some extent, dependent upon assembly clearances, by tension in the chamber producing pressure of the nozzle assembly against the rear trap assembly and pressure of the boss within the front of the chamber against the front trap assembly. Thermal expansion of the tie rods and chamber may release the grains. If a grain becomes displaced an asymmetric flow condition exists resulting in increased propellant erosion or other anomalies which change the thrust. Presuming the chamber not to be contributing to the clamping because of loose assembly and thermal expansion, the tie rod clamping the rear grain may be expected to expand more rapidly than the forward tie rod because of being subjected to a greater flow of combustion gases, thus permitting displacement of the rear grain first and giving rise to the first thrust fluctuation. Subsequently, the forward tie rod expands sufficiently to permit displacement of the forward grain giving rise to the second observed thrust fluctuation.

Camera Studies of Launchings

Sequence photographs of the launching and initial part of the flight with the corresponding time are shown in figure 12. A study of enlargements of these photographs did not reveal any irregularities or indications that propellant failure occurred.

CONCLUSIONS

The flight test of the Aerojet 7KS-6000 T-27 Jato rocket-motor model indicated the following:

1. The maximum absolute longitudinal acceleration imposed upon the rocket in the test was 9.8g and occurred 2.8 seconds after launching.

2. The maximum thrust developed was 7200 pounds, and occurred 4.8 seconds after launching.

3. The total impulse was 43,400 pound-seconds, and the thrusting time was 7.58 seconds.

4. The total impulse is in good agreement and the variation of thrust in general agreement with static tests conducted by the manufacturer and the Aberdeen Proving Ground.

5. No thrust anomalies attributable to effects of flight longitudinal acceleration were observed.

6. Certain small thrust irregularities occurred in the flight test which appear to correspond to irregularities observed in some static tests and may be attributable to the trap design.

Langley Aeronautical Laboratory
National Advisory Committee for Aeronautics
Langley Air Force Base, Va.

Aleck C. Bond
Aleck C. Bond
Aeronautical Research Scientist

Joseph G. Thibodaux Jr.
Joseph G. Thibodaux, Jr.
Aeronautical Research Scientist

Approved: Robert R. Gilruth
Robert R. Gilruth
Chief of Pilotless Aircraft Research Division

GMF

REFERENCES

1. Anon: Jato Manual, SPIA/M1, The Johns Hopkins Univ., Appl. Phy. Lab., March 1949.

2. Pitkin, Marvin, Gardner, William N., and Curfman, Howard J., Jr.: Results of Preliminary Flight Investigation of Aerodynamic Characteristics of the NACA Two-Stage Supersonic Research Model RM-1 Stabilized in Roll at Transonic and Supersonic Velocities. NACA RM L6J23, 1947.

3. Anon: Survey of Bumblebee Activities. Bumblebee Rep. No. 70, The Johns Hopkins Univ., Appl. Phys. Lab., Nov. 1947.

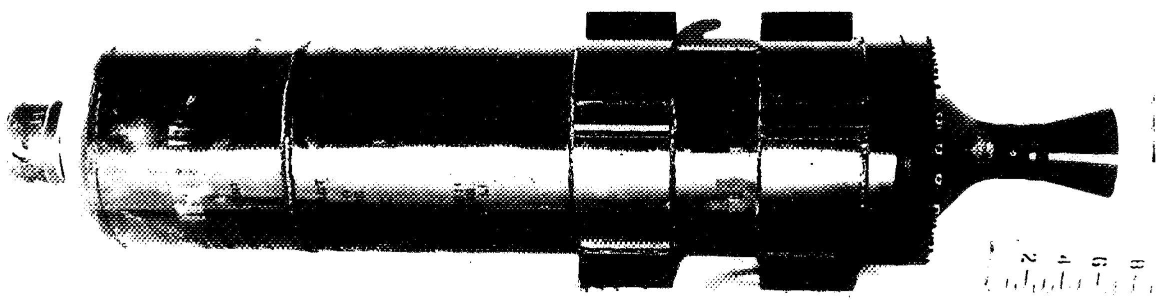

L-61892

(a) Complete unit as supplied by manufacturer.

Figure 1.- Aerojet 7KS-6000 T-27 Jato rocket motor.

[redacted]

[redacted]

1. Capscrews and washers for nozzle assembly.
2. Nozzle assembly with igniter leads.
3. Gasket.
4. Motor body.
5. Ring assembly.
6. Gasket for ring assembly.
7. Retaining sleeve.
8. Gasket for retaining sleeve.
9. Motor body thread protector.
10. Closing cap gasket.
11. Closing cap assembly.
12. Propellant.
13. Propellant.
14. Igniter assembly.
15. Nut for rear trap assembly.
16. Rear trap assembly.
17. Center trap assembly with tie rods.
18. Front trap assembly.
19. Nut for front trap assembly.

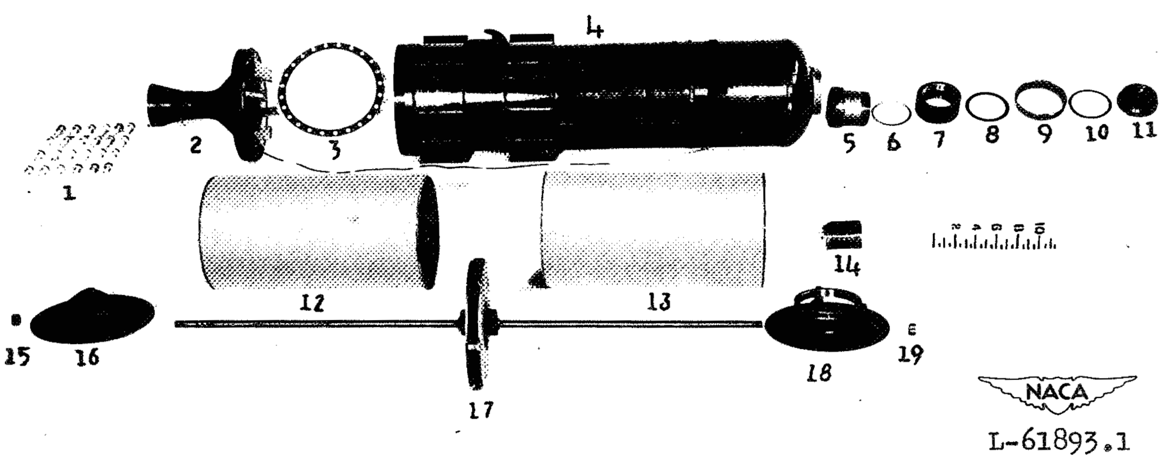

(b) Component parts.

Figure 1.- Concluded.

[redacted]

[redacted]

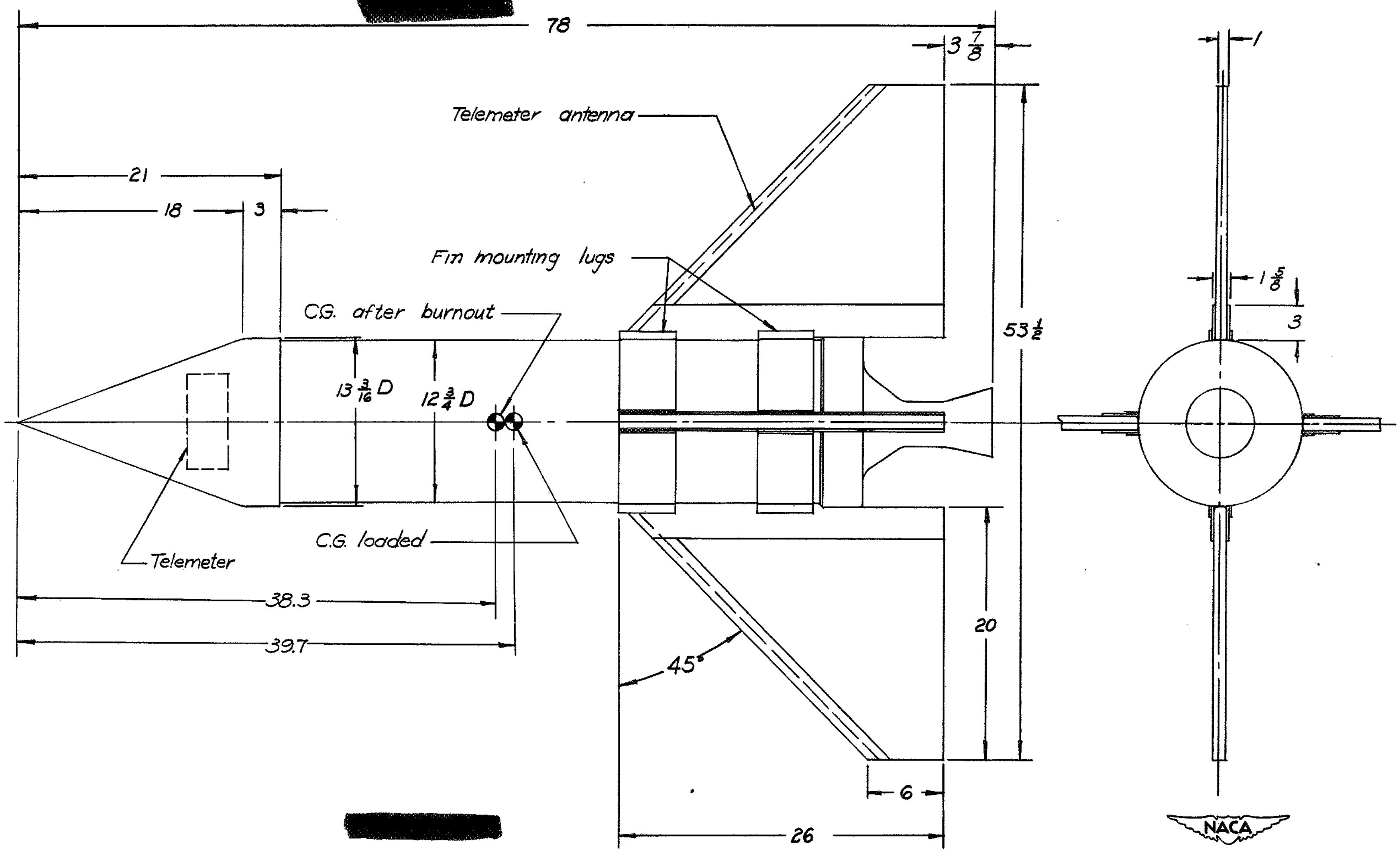

[redacted]

Figure 2.- External configuration of Aerojet Jato 7KS-6000 T-27 rocket-motor flight model. All dimensions are in inches.

[redacted]

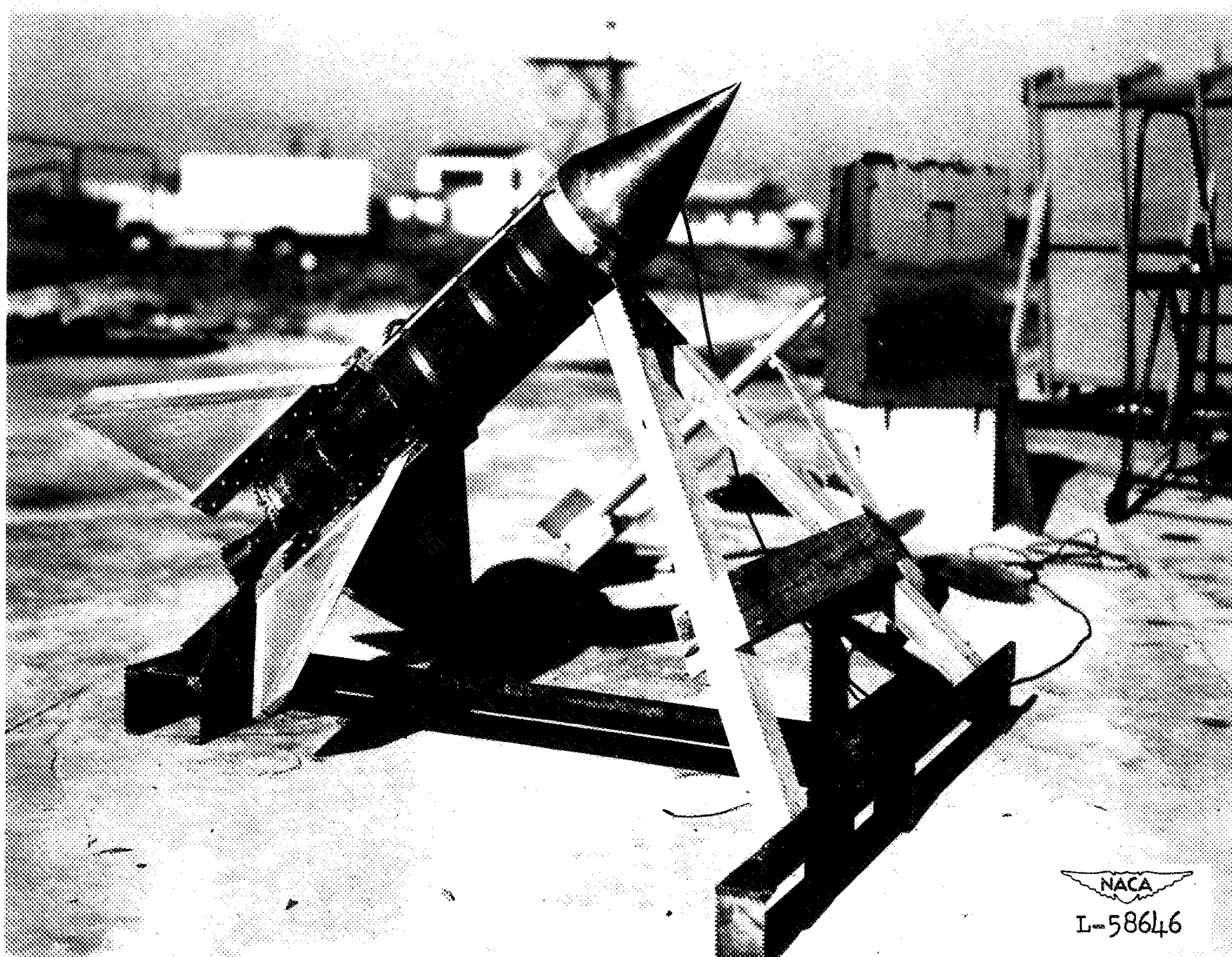

Figure 3.- Aerojet 7KS-6000 T-27 Jato rocket motor. Flight model on launcher.

[redacted]

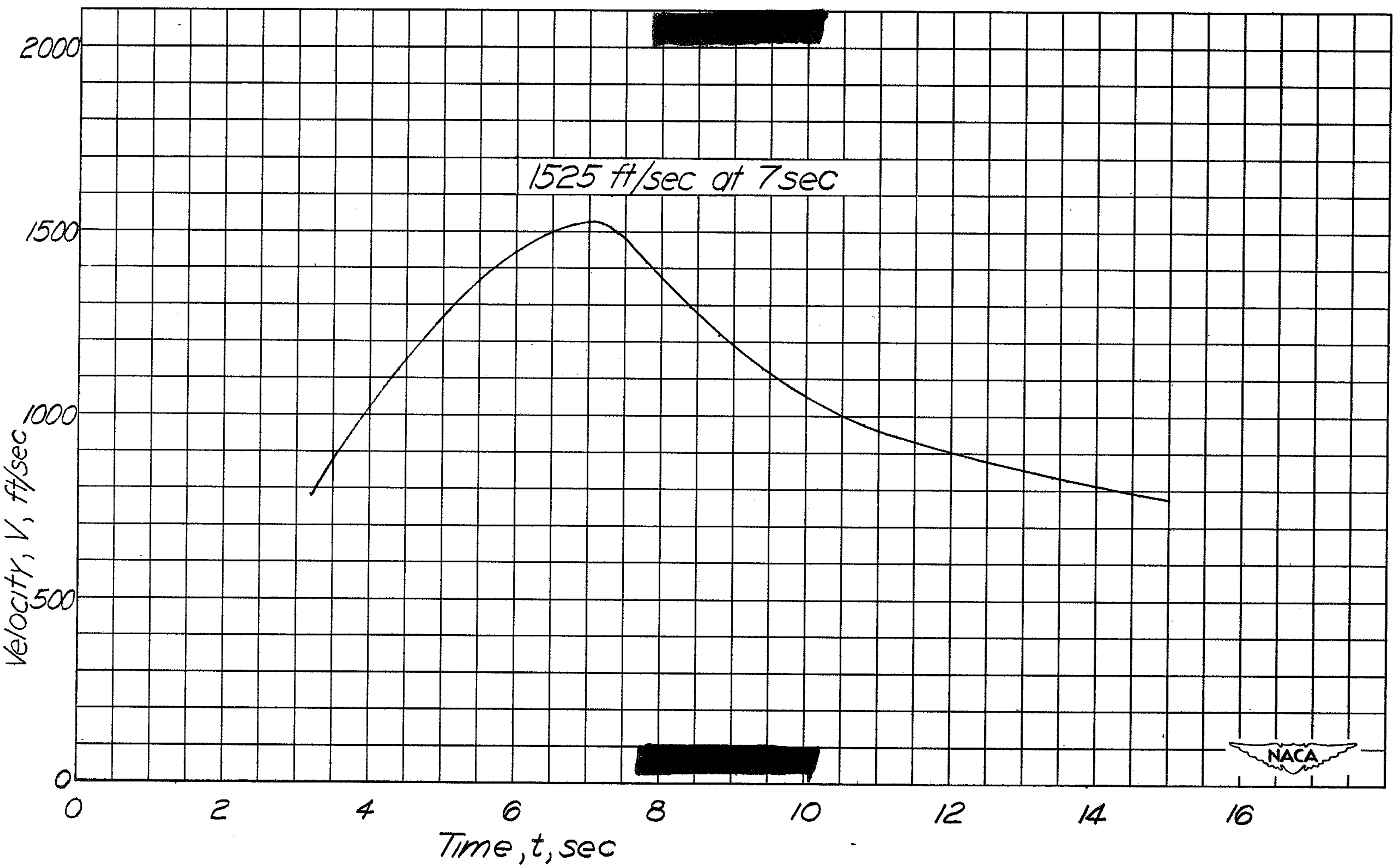

Figure 4.- Velocity-time curve, Aerojet Jato 7KS-6000 T-27 flight model.

[redacted]

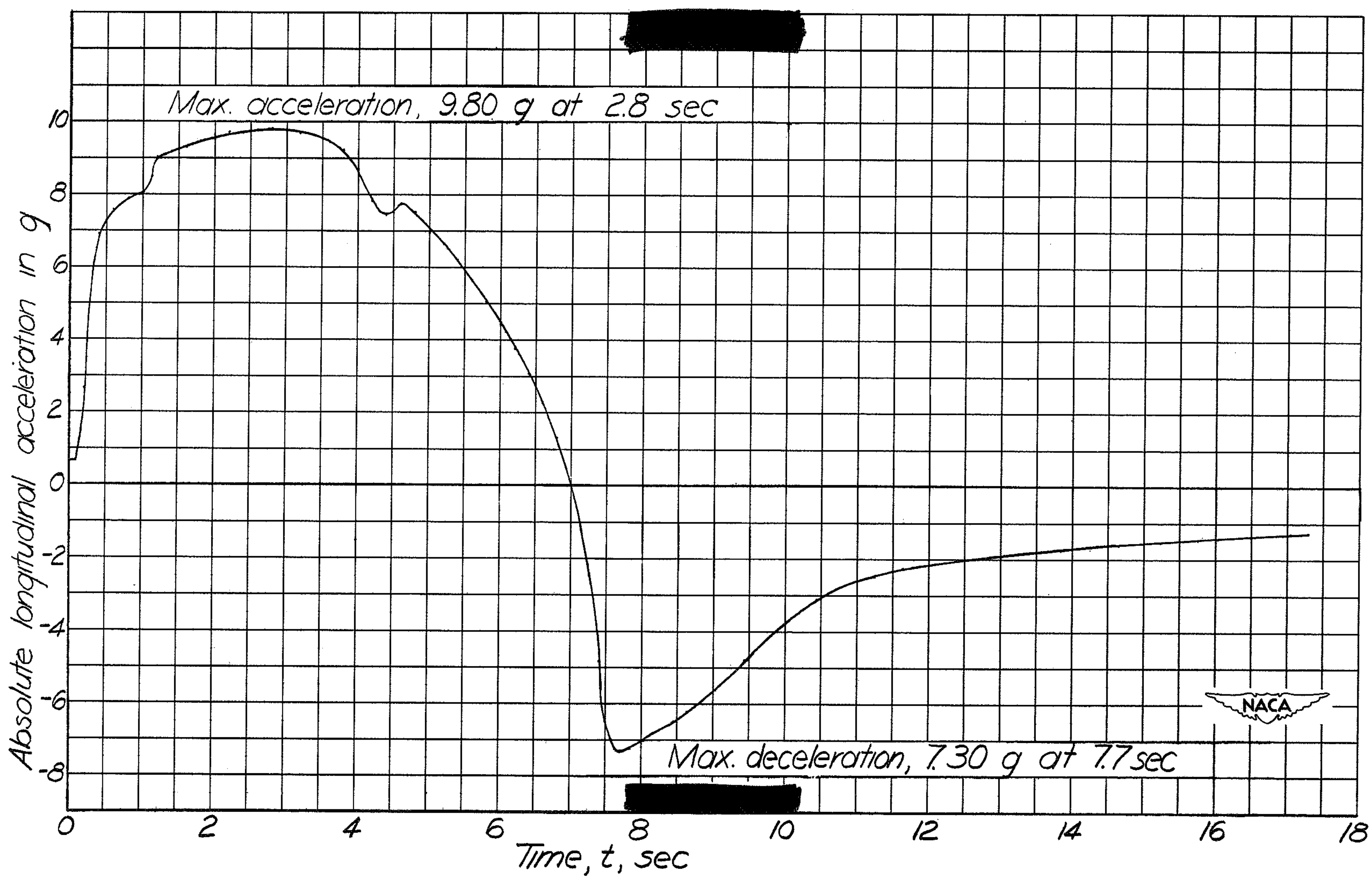

[redacted]

Figure 5.- Acceleration-time curve, Aerojet Jato 7KS-6000 T-27 flight model.

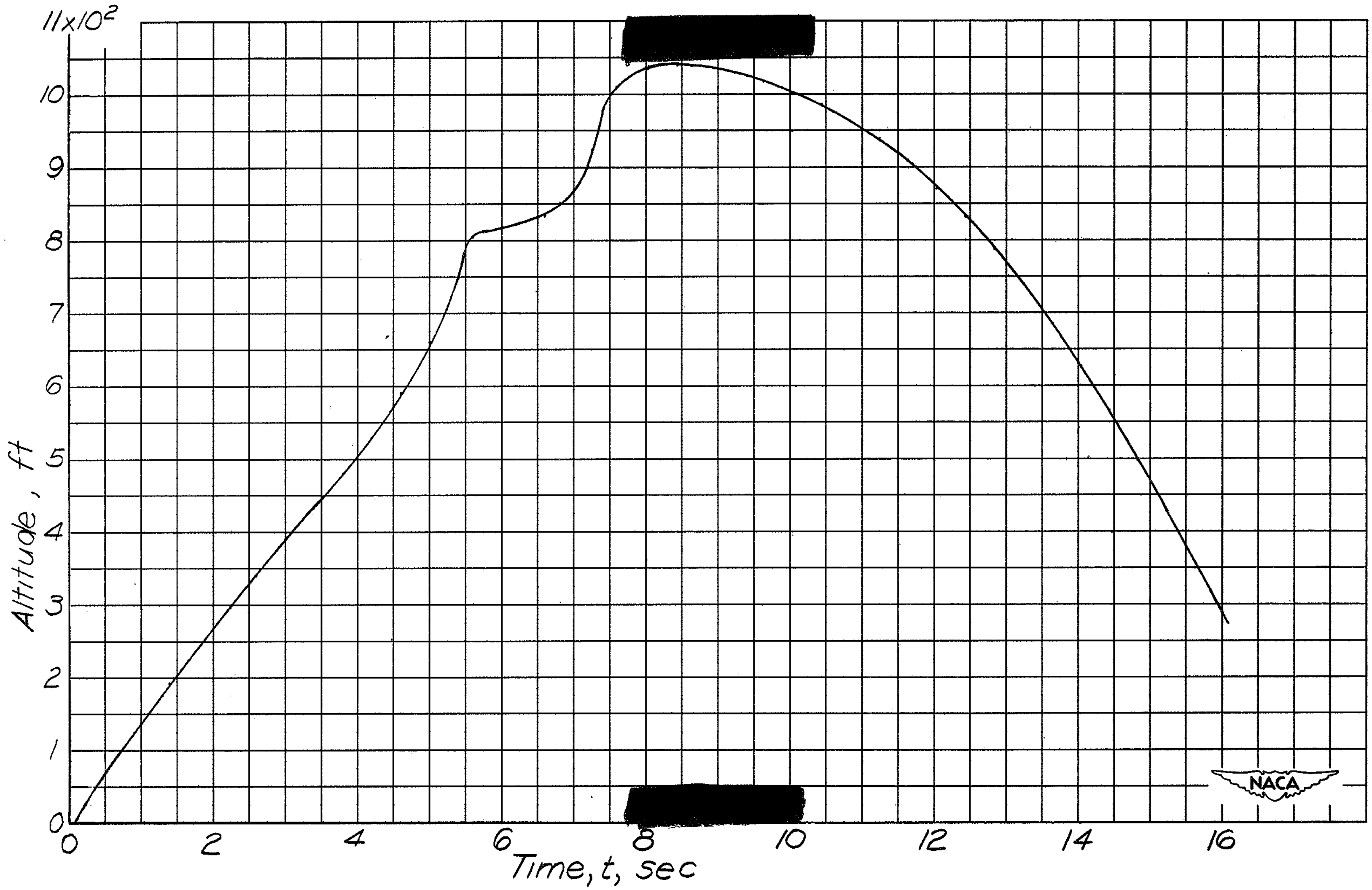

Figure 6.- Altitude-time curve, Aerojet Jato 7KS-6000 T-27 flight model.

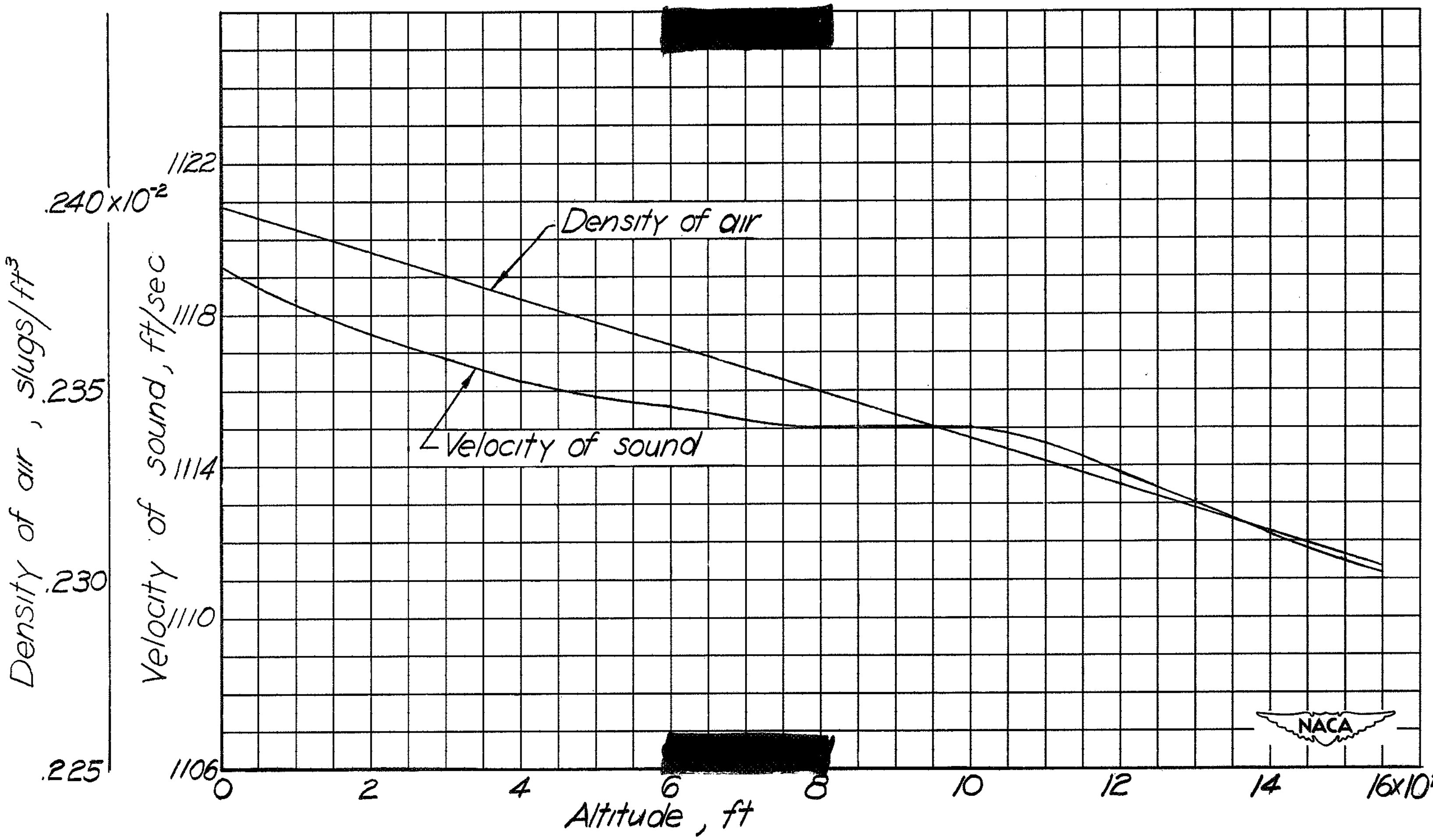

Figure 7.- Variation of density of air and velocity of sound with altitude.

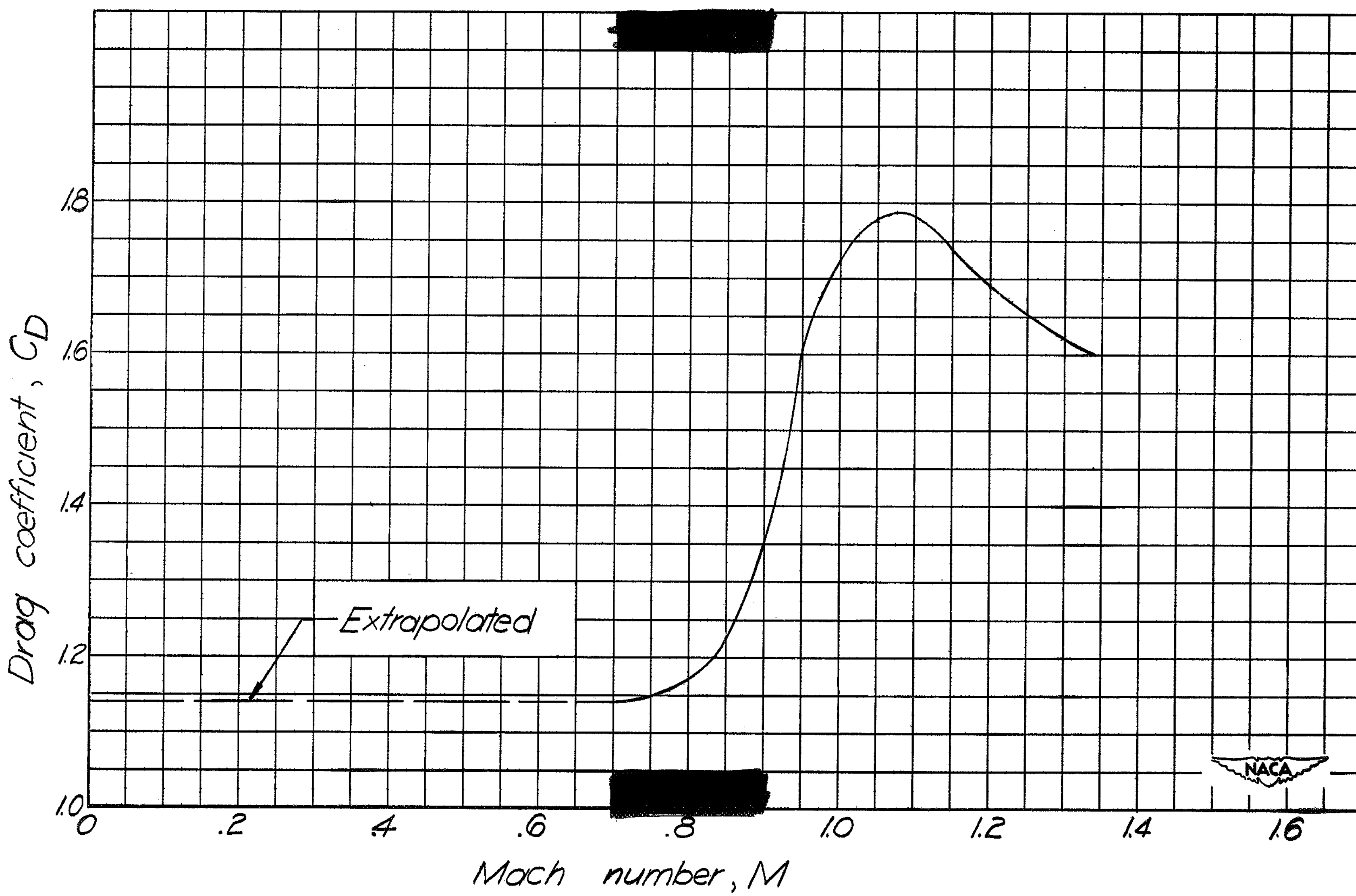

Figure 8.- Variation of drag coefficient with Mach number for Jato 7KS-6000 T-27 flight model.

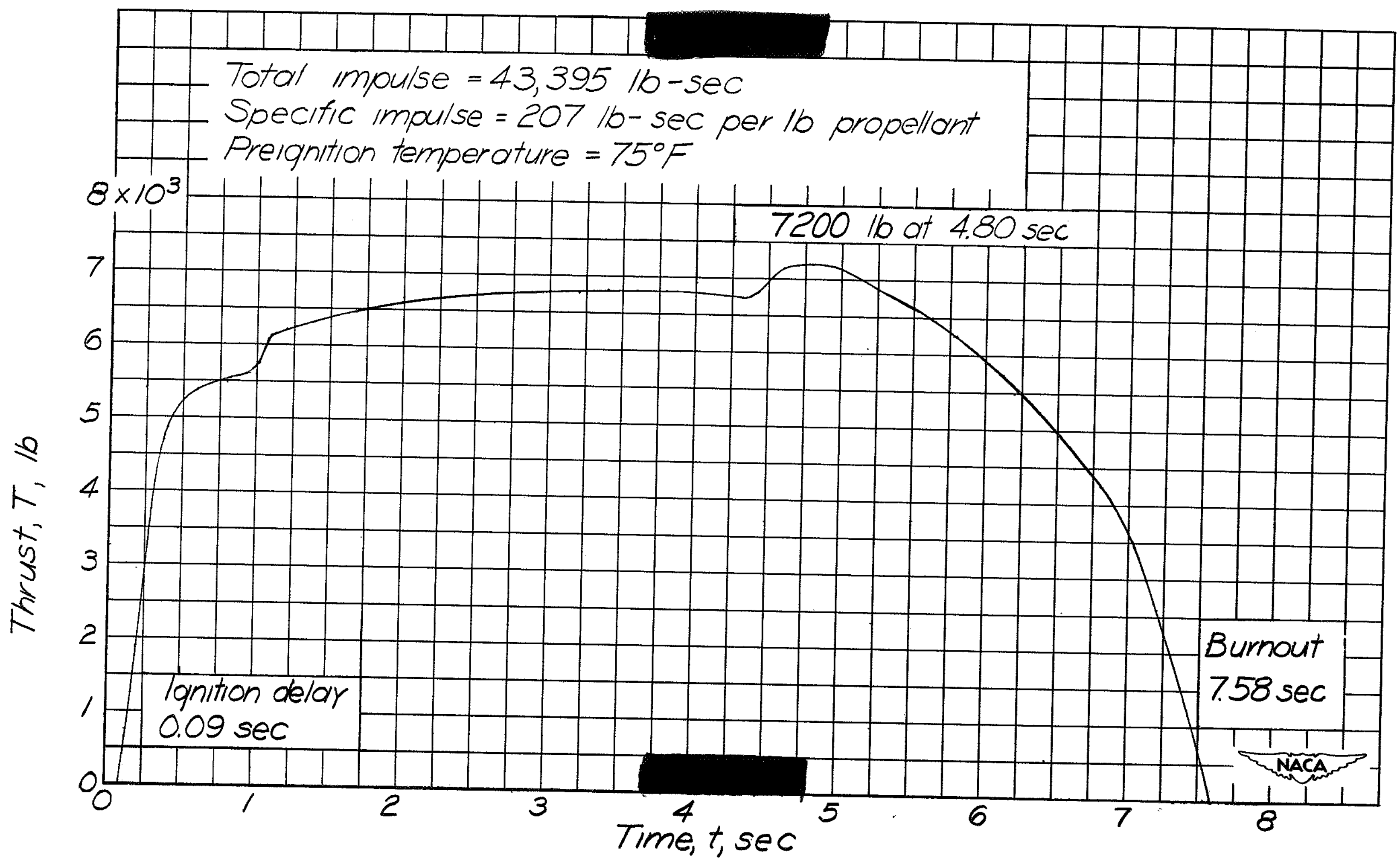

Figure 9.- Thrust-time curve, Aerojet Jato 7KS-6000 T-27 flight model.

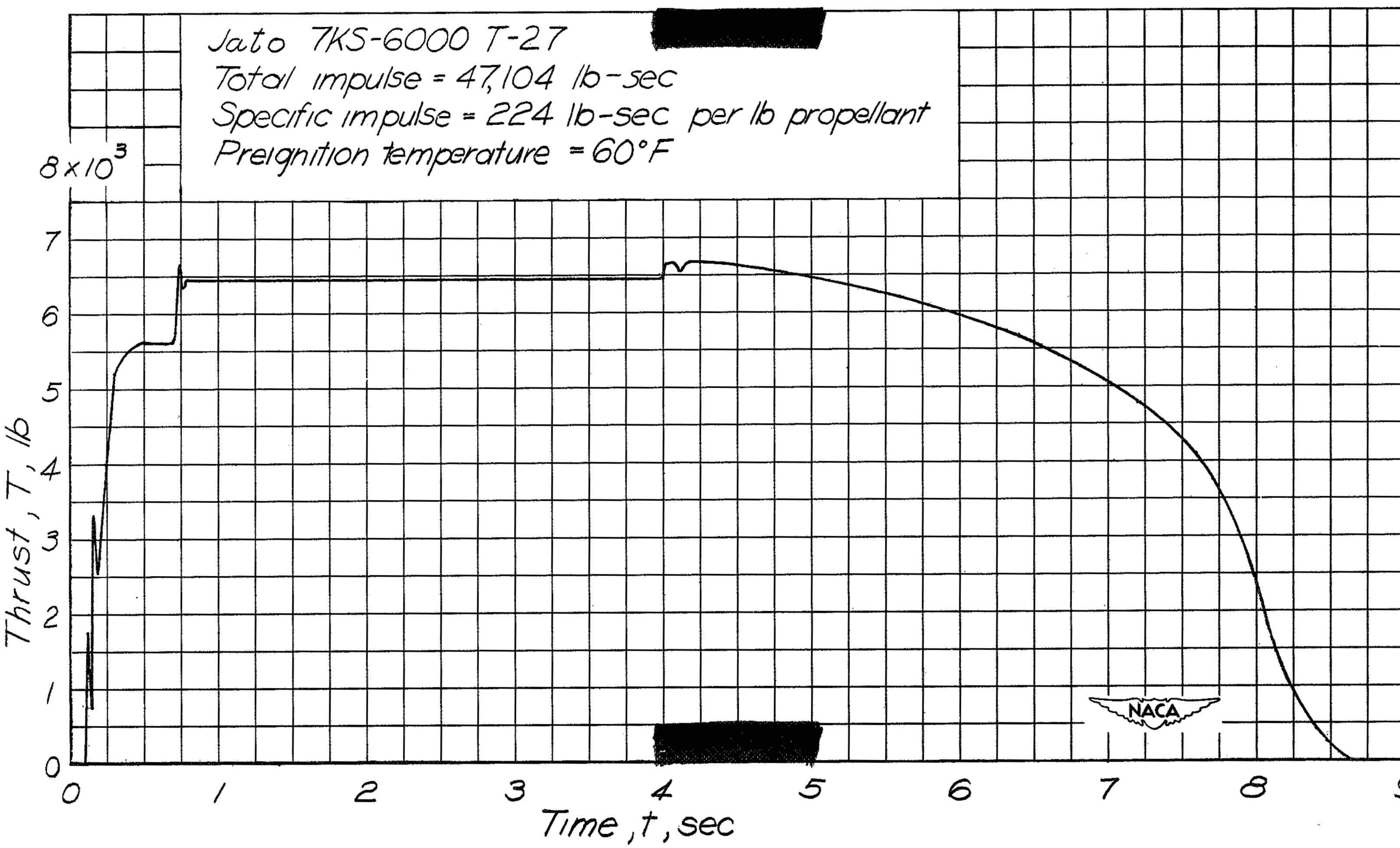

(a) Test 64SM-66.

Figure 10.- Thrust-time curves obtained from static tests by the manufacturer.

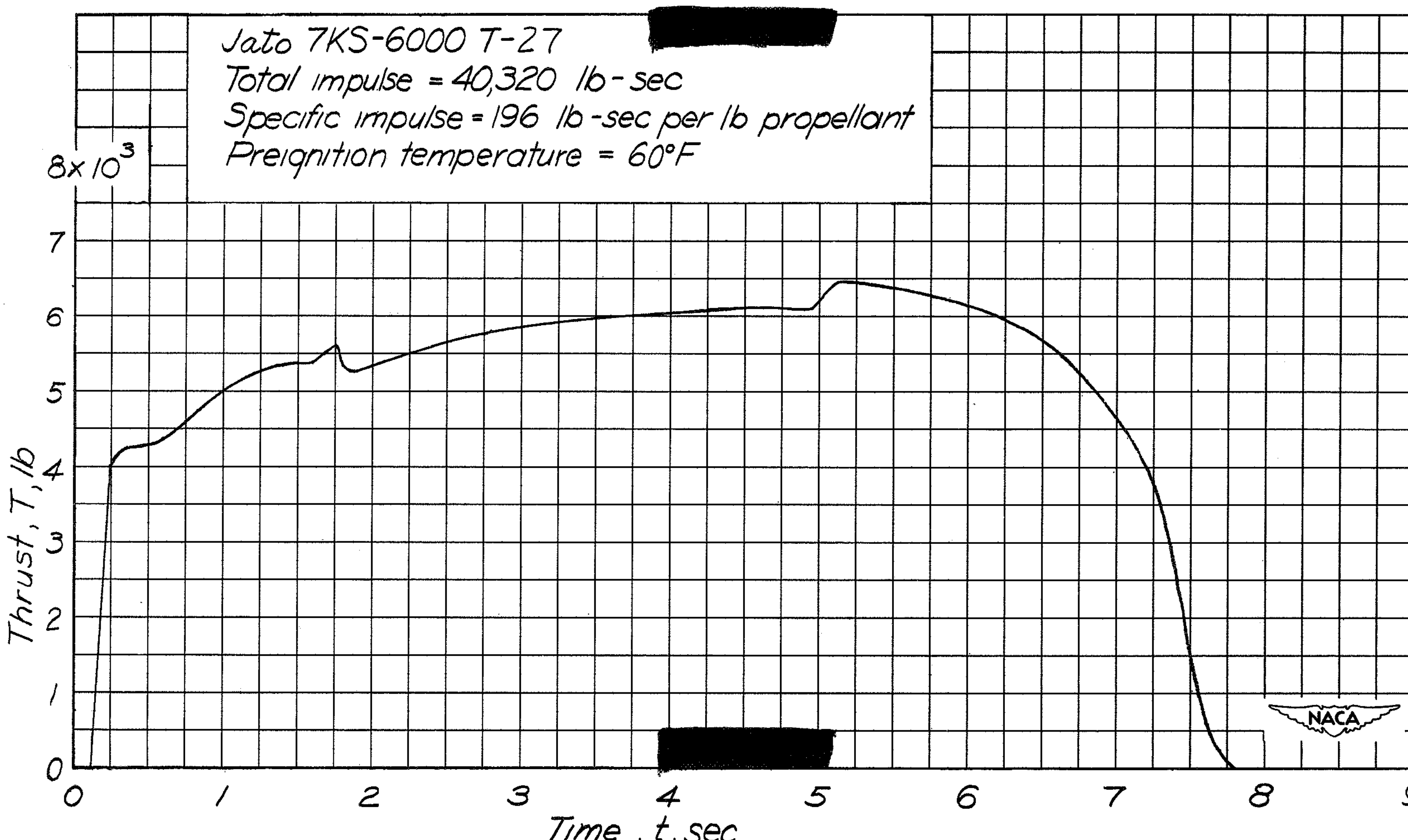

(b) Test 64SM-67.

Figure 10.- Concluded.

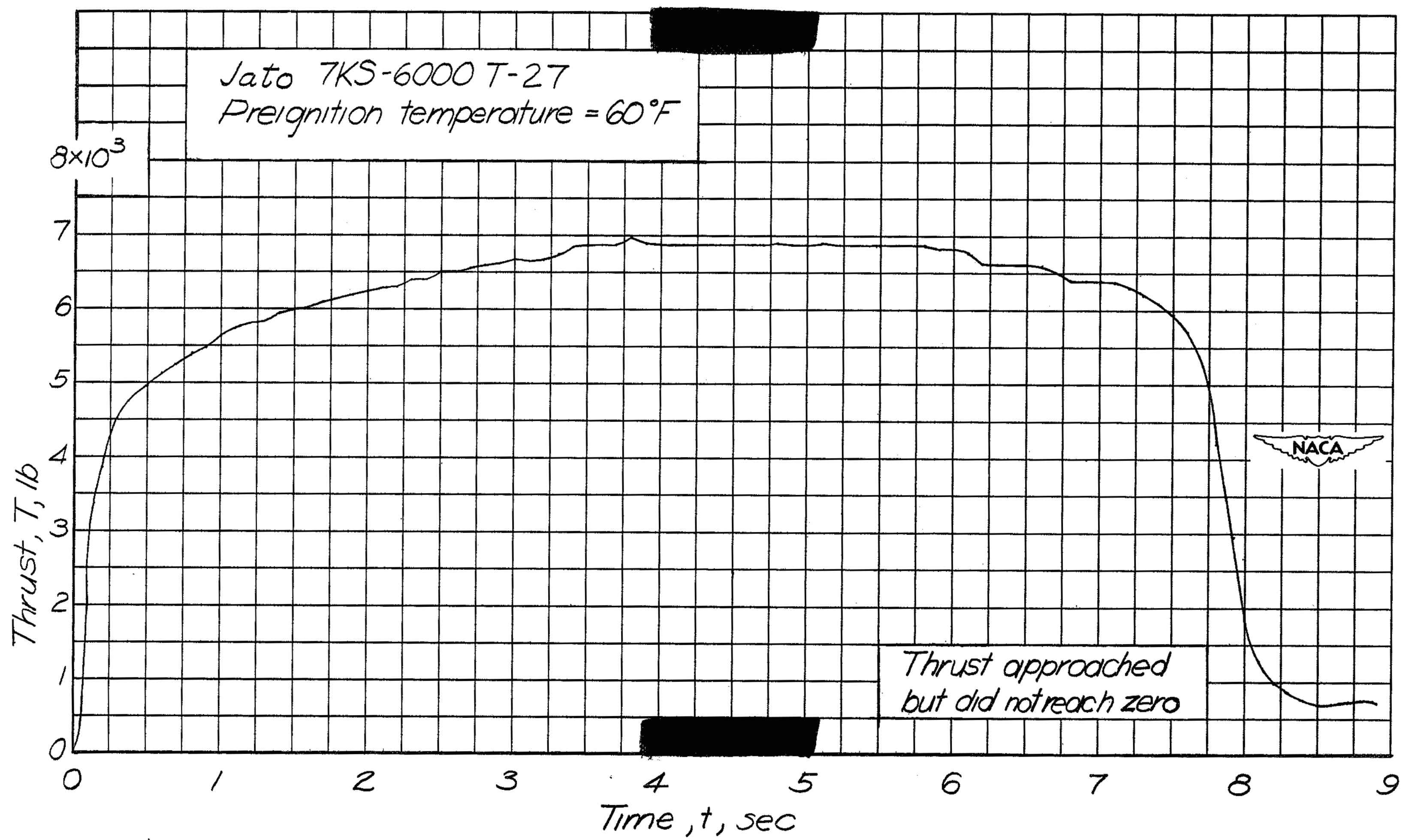

Figure 11.- Thrust-time curve obtained from static tests by the Aberdeen Proving Ground. Round 2, fired January 22, 1948.

[redacted]

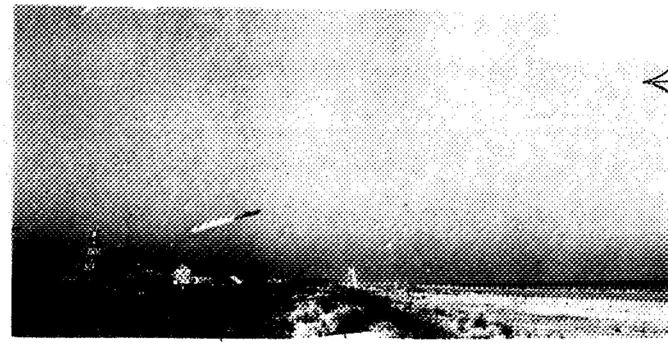

t = 0.38 sec

t = 0.25 sec

t = 0.05 sec

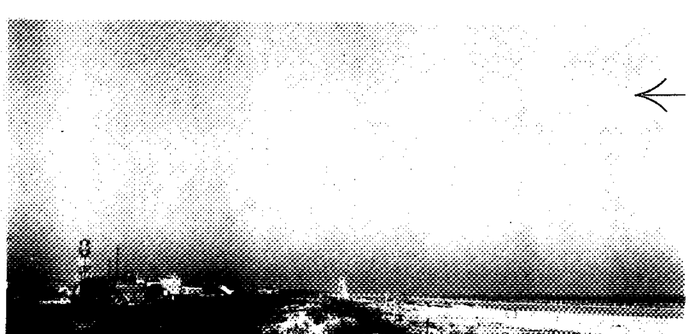

t = 0.00 sec

L-59006

Figure 12.- Sequence photographs of take-off of Aerojet 7KS-6000 T-27 Jato rocket-motor flight model.

[redacted]

[redacted]

t = 1.04 sec

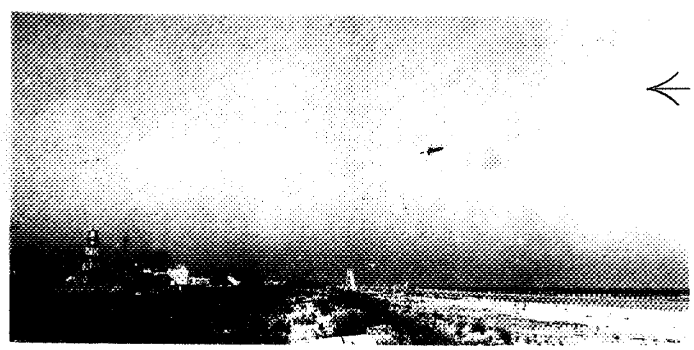

t = 0.71 sec

t = 0.58 sec

NACA
L-59007

Figure 12.- Concluded.

[redacted]